the plant journal

SEB SOCIETY FOR EXPERIMENTAL BIOLOGY

The Plant Journal (2009) **58**, 618–628 doi: 10.1111/j.1365-313X.2009.03802.x

Natural variation in maize architecture is mediated by allelic differences at the PINOID co-ortholog *barren inflorescence2*

Gael Pressoir[1,†,‡], Patrick J Brown[1,†], Wenyan Zhu[1], Narasimham Upadyayula[2], Torbert Rocheford[2], Edward S Buckler[2,3] and Stephen Kresovich[1,*]

[1]*Institute for Genomic Diversity, Cornell University, Ithaca, NY 14853, USA,*

[2]*Department of Crop Sciences, University of Illinois, Urbana, IL 61801, USA, and*

[3]*USDA-ARS*

Received 14 November 2008; revised 29 December 2008; accepted 9 January 2009; published online 23 February 2009.

[*]For correspondence (fax +607 254 6379; e-mail sk20@cornell.edu).

[†]These authors contributed equally.

[‡]Present address: CHIBAS, Port-au-Prince, Haiti.

SUMMARY

We characterized allelic variation at *barren inflorescence2* (*bif2*), a maize co-ortholog of the Arabidopsis PINOID protein kinase (*PID*), and tested for trait associations with *bif2* in both an association mapping population of 277 diverse maize inbreds and in the inter-mated B73 × Mo17 (IBM) linkage population. Results from the quantitative analyses were compared with previous reports of *bif2* phenotypes in mutagenesis studies. All three approaches (association, linkage, and mutagenesis) detect a significant effect of *bif2* on tassel architecture. Association mapping implicates *bif2* in an unexpectedly wide range of traits including plant height, node number, leaf length, and flowering time. Linkage mapping finds a significant interaction effect for node number between *bif2* and other loci, in keeping with previous reports that *bif2*;*spi1* and *Bif2*;*Bif1* double mutants produce fewer phytomers. The Mo17 allele is associated with a reduced tassel branch zone and shows lower expression than the B73 allele in hybrid B73–Mo17 F_1 inflorescences, consistent with the complete absence of tassel branches in the *bif2* knockout mutant. Overall, these data suggest that allelic variation at *bif2* affects maize architecture by modulating auxin transport during vegetative and inflorescence development.

Keywords: *barren inflorescence2*, association mapping, quantitative trait loci, polar auxin transport.

INTRODUCTION

Auxin plays a fundamental role in plant morphogenesis. Beginning with the first zygotic division, auxin transport from the basal to the apical cell establishes an auxin gradient that defines the apical–basal axis (Friml *et al.*, 2003), and the directional transport of auxin is a nearly universal feature of all subsequent events in plant development (Leyser, 2005; Tanaka *et al.*, 2006; Smith, 2008). Polar auxin transport is made possible by the chemical properties of the auxin molecule and the behavior of the proteins that transport it. Since auxin is a weak acid ($pK_a = 4.8$), it is charged and membrane-impermeable within plant cells and is dependent on the activity of efflux carriers for transport (Goldsmith and Goldsmith, 1981). The best understood efflux carriers are the PINFORMED (PIN) class of proteins, which show polar localization and influence the overall direction of auxin transport in plant tissues (Petrasek *et al.*, 2006; Wisniewska *et al.*, 2006). The PIN proteins also cycle dynamically from apical to basal ends of the plasma membrane through vesicle trafficking (Kleine-Vehn *et al.*, 2008), changing the flow of auxin in response to environmental and developmental cues, and are upregulated by auxin (Vieten *et al.*, 2005), permitting the establishment of positive-feedback loops in which auxin is progressively 'canalized' into regions of high concentration (Wenzel *et al.*, 2007). These PIN-mediated auxin fluxes have proven responsible for a wide range of phenomena, including tropism (Friml *et al.*, 2002), phyllotaxis (Reinhardt *et al.*, 2003; Smith *et al.*, 2006), and vascular patterning (Scarpella *et al.*, 2006). Given the intricacy and near ubiquity of this system of auxin distribution in plant development, it has probably played a role in the

evolution and diversification of plant form. However, there is little evidence linking natural variation in the polar auxin transport machinery with plant phenotypic diversity.

Much of the plant shoot is derived from lateral organs produced by the shoot apical meristem. The formation of new lateral organ primordia in Arabidopsis is preceded by the accumulation of auxin in discrete maxima along the meristem flanks (Benkova *et al.*, 2003), which appear to result from changes in PIN1 expression and polarity. The establishment of a new primordium is marked first by PIN1 upregulation and auxin accumulation (Heisler *et al.*, 2005), and then by a reversal in PIN1 polarity which diverts auxin away from the existing primordium towards a new, incipient one (Heisler *et al.*, 2005). This reversal in PIN1 polarity is regulated by its phosphorylation status, which is competitively influenced by two genes: the serine/threonine kinase PINOID (PID; Friml *et al.*, 2004) and the PP2A phosphatase (Michniewicz *et al.*, 2007). *pid* mutants undergo an apical-to-basal shift in PIN1 polarity, whereas *pp2aa* mutants and 35S:*PID* lines have the opposite phenotype (Friml *et al.*, 2004; Michniewicz *et al.*, 2007), and protein extracts from *pp2aa* and *35S:PID* plants are similarly enhanced in their ability to phosphorylate PIN1 *in vitro* (Michniewicz *et al.*, 2007).

The role of PIN proteins in polar auxin transport appears to be fundamentally similar in Arabidopsis and maize (*Zea mays*). Maize contains three PIN1-like genes, *ZmPIN1a*, *ZmPIN1b*, and *ZmPIN1c*, which map to chromosomes 9, 5, and 4 respectively, and are broadly expressed across vegetative and inflorescence development (Gallavotti *et al.*, 2008a). Transformation of Arabidopsis *pin1-3* mutants with a *pAtPIN1::ZmPIN1a* construct is sufficient to fully rescue the branching defects of *pin1-3*, suggesting that ZmPIN1a is a functional auxin efflux carrier (Gallavotti *et al.*, 2008a), and lateral organ formation in maize, as in Arabidopsis, is preceded by a discrete area of *ZmPIN1a* upregulation (Gallavotti *et al.*, 2008a). No *ZmPIN1* mutants have been isolated, probably because of functional redundancy between paralogs.

A maize co-ortholog of Arabidopsis PID is a gene called *barren inflorescence2* (*bif2*), which shows reduced formation of all axillary structures including tassel branches, spikelets, and ear shoots (McSteen and Hake, 2001). This is similar to the phenotype of Arabidopsis PIN and PID mutants, which have pin-like inflorescences resulting from the failure to form floral meristems (Galweiler *et al.*, 1998; Christensen *et al.*, 2000). Maize does not normally show much outgrowth of vegetative branches (tillers), but the *teosinte branched1* (*tb1*) mutation causes plants to tiller profusely, and the reduction in tiller number observed in *bif2;tb1* double mutants compared with *tb1* mutants confirms that *bif2* affects vegetative, as well as inflorescence, axillary meristems (McSteen *et al.*, 2007). Although the *bif2* mutant displays a slight reduction in leaf number in a B73 inbred background (McSteen *et al.*, 2007), it does not suffer from other obvious vegetative defects.

Several other maize mutants have phenotypes similar to *bif2*, including *barren stalk1* (*ba1*), *sparse inflorescence1* (*spi1*), and *Barren inflorescence1* (*Bif1*). *ba1* encodes a basic helix–loop–helix (bHLH) transcription factor necessary for axillary meristem development (Gallavotti *et al.*, 2004). *ba1* interacts with *bif2* in the nucleus and is phosphorylated by *bif2 in vitro* (Skirpan *et al.*, 2008), so it is likely that the phenotypic effects of *bif2* do not result entirely from its role in PIN1 phosphorylation. Moreover, double mutants of *bif2* with *spi1* and *Bif1* have dramatic vegetative phenotypes not seen in any of the corresponding single mutants. The double mutant of *bif2* and *spi1*, which is a member of the YUCCA family of flavin monooxygenases involved in auxin biosynthesis (Gallavotti *et al.*, 2008b), is only half the height of wild-type or single mutant plants and shows a large reduction in leaf number. Similarly, the double mutant of *bif2* and the uncloned *Bif1* locus, which appears to be a regulator of auxin transport (Barazesh and McSteen, 2008), shows a dramatic reduction in both plant height and leaf number. In Arabidopsis, functional redundancy between most YUC proteins requires the construction of double, triple, or quadruple mutants before any phenotypic effect becomes evident (Cheng *et al.*, 2006), whereas in maize the *spi1* mutation alone is able to produce a phenotype (Gallavotti *et al.*, 2008b). Moreover, quadruple *yucca* mutants in Arabidopsis are bushy with increased vegetative branching (Cheng *et al.*, 2006), whereas *spi1; tb1* double mutants in maize have fewer tillers (Gallavotti *et al.*, 2008b). Therefore, although the overall function of the PIN-based auxin transport system is clearly conserved across monocots and dicots, the individual components of this system appear to vary both in genetic redundancy and in their actual effects.

The extent to which differences in auxin synthesis, transport, and response contribute to natural phenotypic variation within and between plant species is impossible to resolve through mutant analysis alone. Natural selection acts upon variation segregating within populations, so dramatic mutant phenotypes are not necessarily of evolutionary significance (Stern, 2000). However, since qualitative mutant alleles and 'wild-type' alleles at quantitative trait loci could simply represent different values along a spectrum of possible allelic effects, mutant phenotypes may inform the choice of candidate genes underlying quantitative variation (Robertson, 1985). For example, the Arabidopsis CAULIFLOWER (CAL) mutant looks convincingly like cauliflower, suggesting that cauliflower may have evolved from its progenitor through mutation of a CAL ortholog. In this case, a hypothesis generated through mutant analysis was verified by associating allelic differences at the CAL locus with variation in the cauliflory trait across *Brassica oleracea* cultivars (Kempin *et al.*, 1995), providing an example of how mutant variation can help identify alleles with large effects

on natural phenotypic variation. However, it is not clear to what extent mutant variation can help identify those alleles with small quantitative phenotypic effects that are thought to make up most naturally segregating functional variation (Orr, 1998). Maize is an excellent model with which to exploit the complementarity between quantitative and mutant variation, since it is phenotypically and genotypically diverse and possesses an excellent collection of well-characterized mutant lines (http://maizecoop.cropsci.uiuc.edu/).

In this study, we evaluate the *bif2* gene as candidate for natural variation in plant architecture in maize. Two methods of relating phenotype to genotype are used: linkage mapping and association mapping. Linkage mapping typically evaluates the progeny of a cross between two parents, so that a limited number of recombination events and only two parental alleles are captured. In contrast, association mapping evaluates a diverse group of more distantly related individuals, with a concomitant increase in recombination, allelic diversity, and genetic complexity (Flint-Garcia *et al.*, 2003). These approaches are complementary because linkage mapping has low resolution but high power to detect quantitative trait loci (QTL), whereas association mapping has low power but high resolution. A suite of maize architectural traits were phenotyped both in a linkage population, the inter-mated B73–Mo17 (IBM) population of recombinant inbred lines, and in an association panel of 277 diverse maize inbreds (Flint-Garcia *et al.*, 2005), as part of a larger US National Science Foundation (NSF)-funded project (Figure 1; http://www.panzea.org/). Linkage data were used for verification of the association results and to conduct genome-wide tests for epistasis which would not have been feasible in the association study. The combination of classical linkage and association mapping approaches employed here, combined with the insights derived from previous mutagenesis studies, provide a powerful new approach for studying the molecular basis of quantitative phenotypes.

RESULTS

Genotypic variation and linkage disequilibrium at the *bif2* locus

In order to test for the possible association of *bif2* polymorphism with phenotypic variation in maize, we first characterized genotypic variation at the *bif2* locus. Two *bif2* amplicons were sequenced in the association panel of 277 maize inbred lines, one from each end of the gene, yielding 39 nucleotide polymorphisms across 263 lines with reasonably complete data (Figure 2, Table S1 in Supporting Information). Although the complete gene sequence of *bif2* was not obtained for all 277 lines, polymorphisms from the 5′ and 3′ ends of the gene are in linkage disequilibrium (LD) with each other (Figure 2), meaning that the state of a single nucleotide polymorphism (SNP) at the 5′ end is correlated with the state of a SNP at the 3′ end. This is significant, because it implies that potential polymorphisms in the unsequenced middle portion of the gene will be correlated

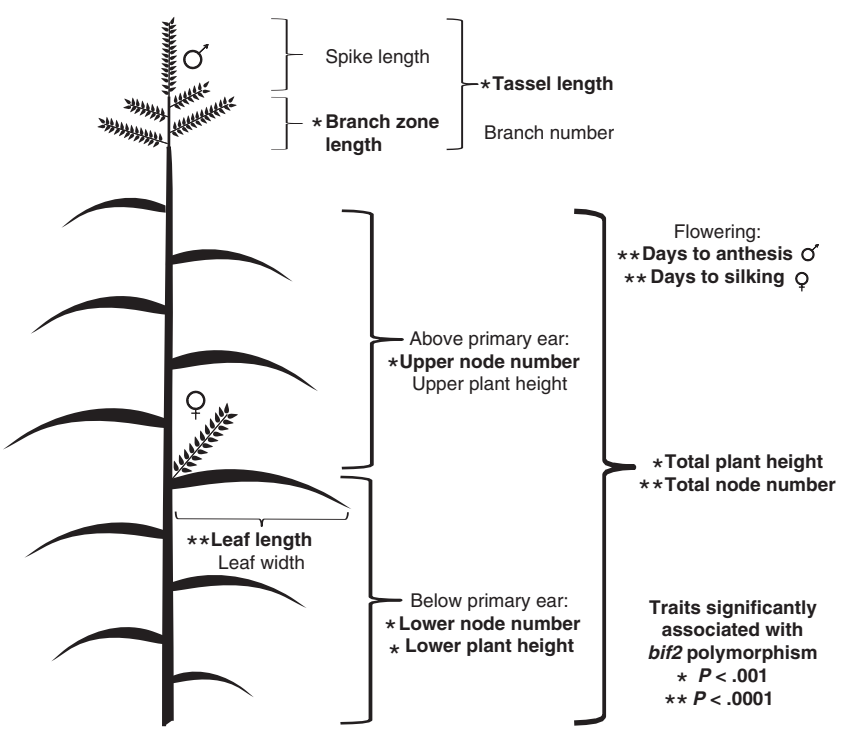

Figure 1. The 14 maize traits phenotyped in this study.
The primary ear is the largest, uppermost ear. Leaf length and width were measured on the leaf blade subtending the primary ear.

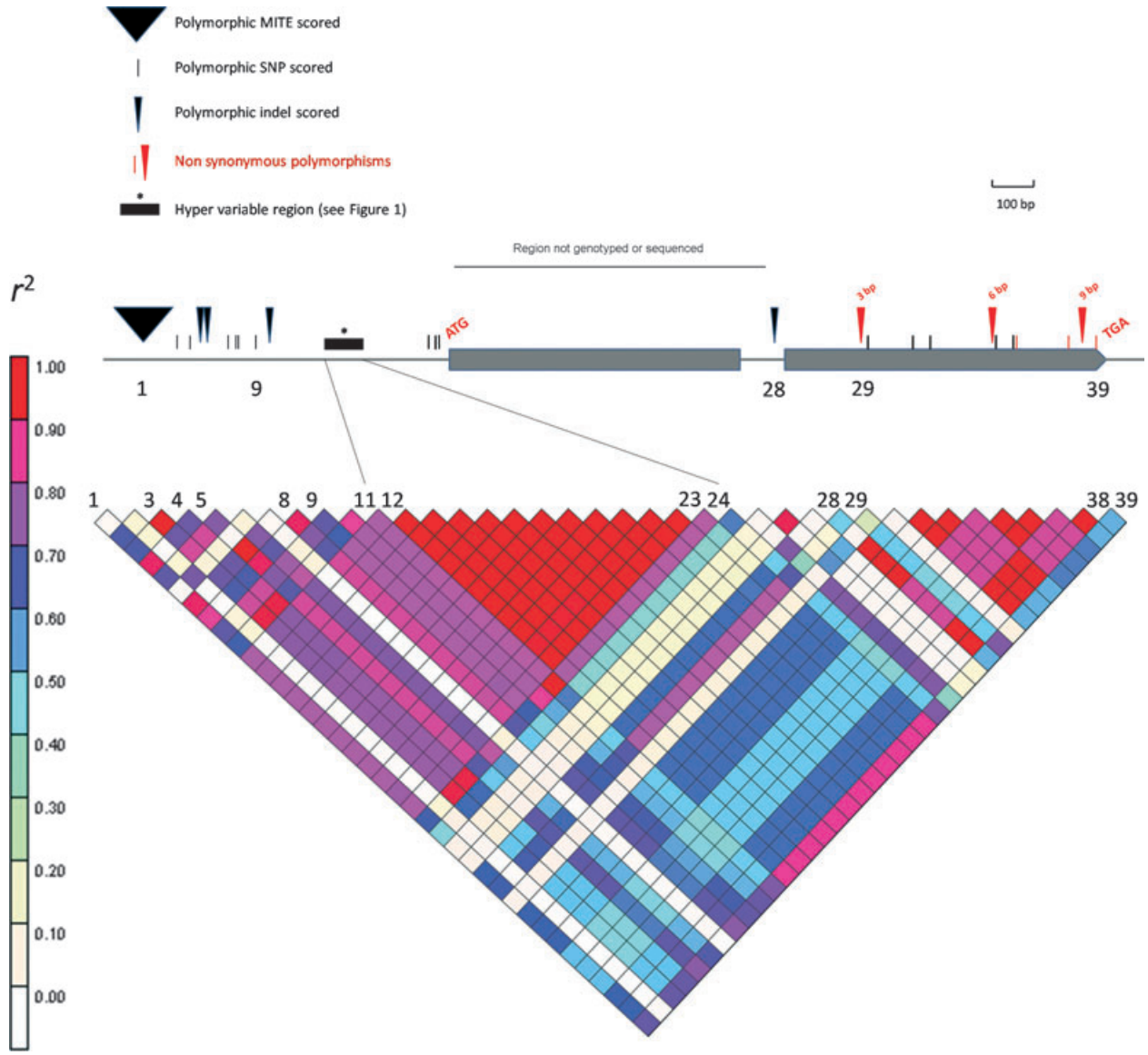

Figure 2. Linkage disequilibrium at the *bif2* locus.
Polymorphic sites are positioned along the *bif2* gene. The colored boxes indicate the correlation r^2 or linkage disequilibrium between pairs of polymorphisms. An r^2 of 1 is indicative of complete linkage disequilibrium.

with our data. The few lower r^2 values seen in Figure 2 are due to low-frequency SNPs that are still in high LD with higher-frequency SNPs, indicating that there is little evidence for recombination across *bif2*. This is in contrast to most maize genes, which show evidence of substantial intragenic recombination (Remington *et al.*, 2001). Overall, *bif2* has two major haplotype classes, one of which includes B73, and the other Mo17 (Table S1). Two-thirds of the polymorphic sites are upstream of the start codon, including a TTATAA insertion 172 bp upstream of the start codon in B73 (Figure 3). The two haplotype classes are not distributed equally with regard to population structure, which was estimated by assigning each line to Stiff-Stalk, Non-Stiff-Stalk, and Tropical subpopulations (Thornsberry *et al.*, 2001). Lines carrying the TTATAA insertion, for example, average 20% Stiff-Stalk and 43% Non-Stiff Stalk, whereas lines without the insertion average just 6% Stiff-Stalk and 75% Non-Stiff-Stalk (Table S1).

Trait associations with *bif2* polymorphism in a panel of diverse maize inbreds

We tested for association between *bif2* polymorphism and phenotypic variation across a diverse maize sample using a mixed-model approach that controls for false positives using both coarse- and fine-scaled estimates of related-

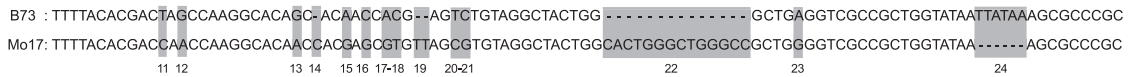

Figure 3. B73–Mo17 sequence alignment of the hypervariable region in the *bif2* promoter.
Polymorphisms 11–24 from Figure 2 are highlighted and numbered below the alignment.

ness (Yu *et al.*, 2006). Since *bif2* polymorphism correlates with population structure, part of the actual effect of *bif2* may be absorbed by the population structure covariates in our model. Nevertheless, *bif2* associates strongly with tassel length (Table 1: $P = 2 \times 10^{-4}$), both male and female flowering time (days to anthesis, $P = 1 \times 10^{-4}$, and days to silk, $P = 3 \times 10^{-5}$), plant height ($P = 4 \times 10^{-4}$), both total and lower node number (total, $P = 9 \times 10^{-5}$; lower, $P = 2 \times 10^{-4}$), and leaf length (LL; $P = 5 \times 10^{-5}$). Although the *bif2* mutant was originally identified by its lack of tassel branches, *bif2* associates only marginally with tassel branch number ($P = 5 \times 10^{-3}$). Total tassel length is the sum of the lengths of the branch zone and spike, and we observe that *bif2* is significantly associated with branch zone length ($P = 1 \times 10^{-3}$) but not spike length ($P > 0.01$). Similarly, we observe that *bif2* associates with node number and plant height predominantly in the lower portion of the plant, below the primary ear, and to a much lesser extent in the upper portion above the primary ear. The SNPs showing strong association with these phenotypes are numerous, spanning the entire length of *bif2*, and are in high LD with one another (Figure 2, Table 1). Variation at *bif2* explains roughly 9–12% of the additive genetic variation for these traits in the association panel. In every case the B73 allele conditions an increase in trait value: this allele is associated with taller, later-flowering plants with longer tassels and leaves and more nodes (Table 2).

Trait associations with the *bif2* region in the IBM linkage population

In order to confirm our association mapping results, we conducted linkage mapping in the maize IBM population using the same set of traits that were measured in the association panel. The parents of the IBM population, B73 and Mo17, represent the two major *bif2* haplotypes and are segregating for most, but not all, of the polymorphisms identified as significant using association mapping (Table 1). We detected QTL for tassel length and tassel branch zone length in the *bif2* region ($P < 1 \times 10^{-3}$; Figure 4a,b). The estimated effects of the B73 allele on tassel length and branch zone length were also remarkably consistent between the association and linkage analyses (Table 2). Since several recent studies have shown that combining the *bif2* mutation with other auxin-related mutations can yield dramatic double mutant phenotypes (Barazesh and McSteen, 2008; Gallavotti *et al.*, 2008b), we then tested every marker for interaction with *bif2* (see Experimental Procedures). Although the individual effect

Table 1 Trait associations [$-\log_{10}$(*P*-value)] with polymorphisms at the *bif2* locus

		Tassel				Flowering		Plant height			Node number			Leaf	
Sites	IBM[a]	Tassel length	Spike length	Branch zone	Branch number	Days to anthesis	Days to silking	Total	Lower[b]	Upper[b]	Total	Lower[b]	Upper[b]	Length	Width
1	Yes	2.01	0.35	2.20	1.64	**4.01**[c]	**4.64**	2.46	2.01	1.28	**3.97**	**3.72**	1.98	2.88	2.03
3–4	Yes	**3.08**	0.96	2.33	1.66	**3.18**	**3.64**	2.65	2.18	1.53	**4.06**	**3.05**	**3.15**	**3.69**	1.01
5, 8	Yes	2.27	0.77	1.60	0.82	**3.32**	**3.71**	2.42	1.79	1.51	**3.30**	2.85	2.13	2.71	1.55
9	Yes	**3.31**	1.17	2.11	0.87	2.74	**3.24**	**3.06**	1.99	2.16	**3.27**	2.81	2.09	2.96	1.35
11, 24	Yes	**3.11**	0.74	2.93	2.26	**3.34**	**3.89**	2.90	2.56	1.37	**3.78**	**3.06**	2.63	**3.91**	1.06
12–15, 22	Yes	**3.67**	1.05	2.88	1.29	**3.74**	**4.18**	**3.40**	2.91	1.46	**3.55**	**3.35**	1.87	**4.24**	2.02
16–21, 23	Yes	**3.67**	1.05	2.90	1.29	**3.77**	**4.22**	**3.42**	2.93	1.47	**3.56**	**3.37**	1.87	**4.31**	2.02
28	No	**3.53**	1.94	1.33	0.37	2.65	3.02	2.45	1.45	2.17	nc[d]	1.99	2.02	**3.23**	1.64
29	Yes	2.13	0.34	2.66	1.38	**3.21**	**3.79**	**3.16**	**3.00**	1.18	2.79	**3.16**	1.00	**3.62**	1.52
31–33, 37–38	No	**3.53**	1.93	1.30	0.35	2.64	3.00	2.42	1.40	2.16	nc	1.96	1.99	**3.22**	1.63
39	Yes	3.18	0.68	**3.00**	1.04	**4.32**	**4.61**	2.61	2.87	0.78	2.81	**3.00**	1.22	**3.63**	1.94

[a]Site polymorphic in the inter-mated B73 × Mo17 (IBM) population?
[b]'Upper' refers to plant height/node number above the primary ear, 'Lower' to plant height/node number below the primary ear, and 'Total' to the sum of Upper and Lower.
[c]Bold values exceed significance threshold of $-\log_{10}$(*P*-value) >3.0 or (*P*-value) <0.001.
[d]nc, mixed model did not converge.

Table 2 Effect estimates of the B73 *bif2* allele from association and linkage mapping

	Tassel		Flowering		Plant height		Node number			Leaf
Population	Tassel length (mm)	Branch zone (mm)	Days to anthesis	Days to silking	Total (cm)	Lower (cm)	Total	Lower	Upper	Length (mm)
Association[a]	22.63 ± 13.29	11.1 ± 7.9	3.62 ± 1.94	4.31 ± 2.13	10.94 ± 6.63	7.21 ± 5.1	1.05 ± 0.54	0.73 ± 0.4	0.35 ± 0.25	52.8 ± 26.84
Linkage[b]	19.01 ± 11.70	9.76 ± 5.42	NS	NS	NS	NS	Epistasis	Epistasis	NS	NS

[a]Evaluated as a contrast between lines with B73 and Mo17 promoter haplotypes.
[b]Evaluated in the B73 × Mo17 (IBM) population.
NS, not significant.

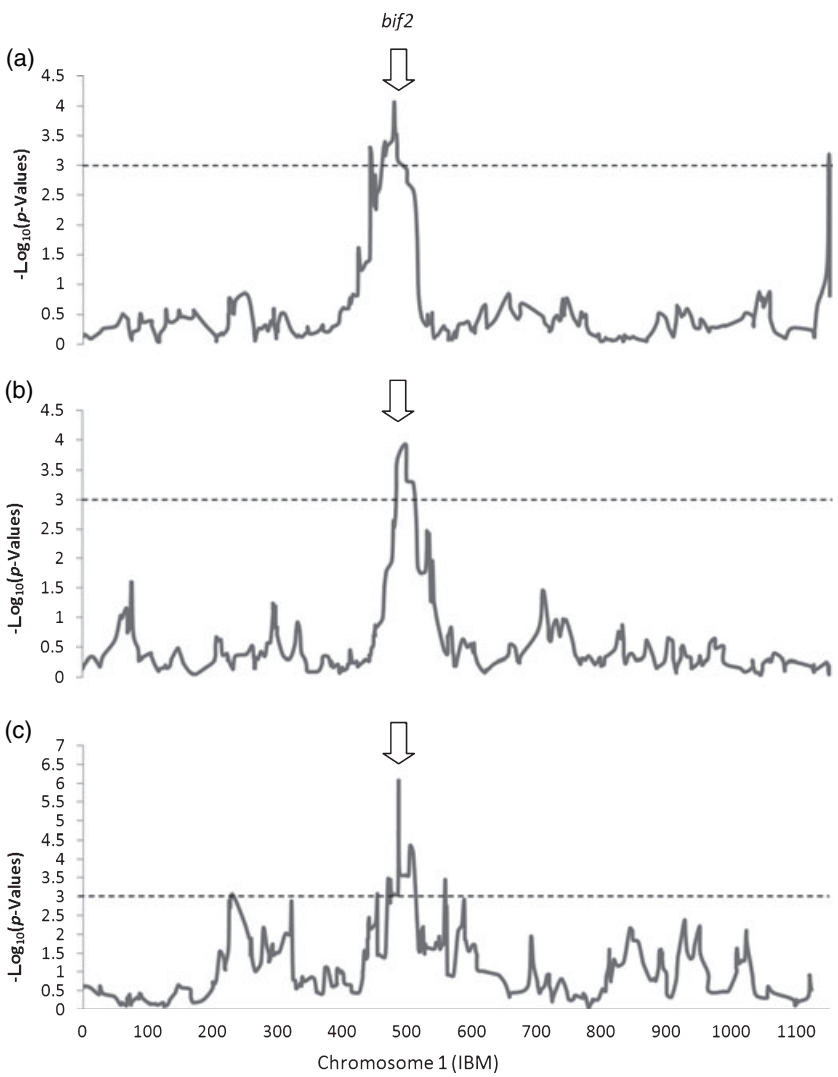

Figure 4. *bif2*-linked quantitative trait loci (QTL) and segregation distortion in the B73 × Mo17 (IBM) population.
(a) The QTL for tassel length using the following markers as cofactors: umc1755 (BIN 2.06), mmp79 (BIN 3.03), ufg56 (BIN 10.06), AY109809 (BIN 7.02), umc1265 (BIN 2.02).
(b) The QTL for tassel branch zone length using the following markers as cofactors: umc1842 (BIN 4.08), umc1822 (BIN 5.05), umc1265 (BIN 2.02), npi449a (BIN 5.04), umc1392 (BIN 3.04), mmp79 (BIN 3.03), bnlg1028 (BIN 10.06).
(c) Segregation distortion. The location of *bif2* in each graph is indicated by an arrow.

of *bif2* on node number was only marginally significant ($P = 2 \times 10^{-3}$), the interaction of *bif2* with two other genomic regions was highly significant for node number in the IBM population (Table 3). Finally, we observed strong segregation distortion in the *bif2* region of the IBM2 map (between umc1601 and umc67a; Fu *et al.*, 2006), with the Mo17 allele present at a significantly lower frequency then expected ($P = 4.55 \times 10^{-7}$; Figure 4c).

Table 3 Quantitative trait loci for node number in B73 × Mo17 (IBM) obtained from stepwise regression

Marker	BIN				$P > F$	$-\text{Log}_{10}$ (P-value)
bnlg1444	BIN 4.08	×	*bif2*	BIN 1.05–1.06	4.53×10^{-11}	10.34
bnlg1429	BIN 1.02				1.47×10^{-9}	8.83
umc1137	BIN 9.07				2.10×10^{-6}	5.68
bnlg1108	BIN 3.08				1.29×10^{-5}	4.89
mmp61	BIN 1.05				5.51×10^{-5}	4.26
bnlg2323	BIN 5.04	×	*bif2*	BIN 1.05–1.06	8.04×10^{-5}	4.09
bnlg1496	BIN 3.09				1.32×10^{-4}	3.88

Expression of B73 and Mo17 *bif2* alleles

Because most of the polymorphism detected at *bif2* is found upstream of the start codon and none of the non-synonymous mutations are in conserved domains, we considered the possibility that the phenotypic effects of *bif2* polymorphism are driven by differences in expression. An allele-specific expression assay was performed to compare the relative expression of B73 and Mo17 *bif2* alleles in F_1 inflorescences (Table 4). The B73 *bif2* allele is consistently expressed at a significantly higher level than the Mo17 allele within the same biological sample. Over all ear and tassel meristems cDNA samples assayed, the average B73/Mo17 expression ratio was 1.402 ± 0.118. This expression bias became more pronounced with increasing meristem size (data not shown), and the ratio was also slightly higher in ears than in tassels. We then performed 5′ and 3′ rapid amplification of 5′/3′ complementary DNA ends (RACE) on *bif2* cDNA isolated from B73–Mo17 F_1 inflorescences. Eight random 5′ clones and eight random 3′ clones were sequenced and identified as belonging to either the B73 or the Mo17 transcript based on previously identified nucleotide polymorphisms. The longest 5′ RACE products from both B73 and Mo17 transcripts initiate 29 bp downstream of the TATAAA element shown in Figure 3. Therefore, there is no evidence for alternative transcription initiation sites as a mechanism for the difference in expression between *bif2* alleles. All 3′ RACE products from the B73 transcript were poly-adenylated 128 bp downstream of the stop codon, whereas the 3′ RACE products from the Mo17 transcript varied in length and were poly-adenylated at sites from 12 bp upstream to 5 bp downstream of the B73 poly-adenylation site.

Table 4 Expression ratio of B73 to Mo17 *bif2* alleles in F_1 inflorescence meristems

	Ear	Tassel	Overall[c]
Average	1.450***	1.283**	1.402***
SD[a]	0.323	0.288	0.317
CI[b]	±0.141	±0.199	±0.118

[a]Standard deviation.
[b]95% confidence interval.
[c]Ear and tassel.
**significantly >1 ($P < 0.01$); ***Significantly >1 ($P < 0.001$).

DISCUSSION

Allelic variation at *bif2* is associated with maize architectural diversity

Polymorphisms at the *bif2* locus show strong association with an unexpectedly wide variety of plant architectural traits including tassel length, plant height, node number, leaf length, and flowering time. The association with tassel length was expected, since tassel morphology is severely affected in a *bif2* mutant background. Similarly, the associations with plant height and node number were not unexpected, since *bif2*;*spi1* and *Bif2*;*Bif1* double mutants have severely reduced plant height and phytomer number (Gallavotti *et al.*, 2008b; Barazesh and McSteen, 2008; node number and leaf number are equivalent proxies for phytomer number). However, the association of *bif2* with variation in flowering time and leaf length was surprising, since these are traits not previously reported to be affected by *bif2*, either alone or in combination with other mutations. Given that *bif2* shows evidence of association with a majority of the traits measured in this study it is possible that additional traits may also be affected by *bif2*. Two specific traits of interest that were not investigated in the current study include ear architecture, which is altered in *bif2* mutants (McSteen and Hake, 2001), and root architecture, which is affected in PID overexpressors (Benjamins *et al.*, 2001).

Only a subset of the trait associations detected in the association panel were confirmed in the IBM linkage population. Main effect QTL were detected only for tassel traits, the effect on node number was highly epistatic, and no effects were detected for flowering time or leaf length, even though the experiment had sufficient power to detect many other QTL of small effect. The expressivity of some phenotypes may be background dependent, such that polymorphisms segregating in additional linkage populations (for example, the set of 25 nested association mapping (NAM) linkage populations; Yu *et al.*, 2008) will be required to elaborate the effect of *bif2* variation on these traits. Also, the segregation distortion observed around the *bif2* locus (Figure 4c) may indicate that allelic combinations with drastic fitness-reducing effects (for example, inability to form ear shoots) have been selected against during the making of the IBM population.

The specific effects of *bif2* polymorphism on tassel architecture did not conform exactly to earlier interpretations of *bif2* effects. We detected QTL and associations with *bif2* for the length of the tassel branch zone (the distance from the lowest to the highest tassel branch) but we detected no QTL and only a weak association for tassel branch number, whereas the *bif2* mutant is characterized by an

absence of tassel branches and the total tassel length from flag leaf to apex is not affected (P. McSteen, Penn State University, PA, USA, personal communication). However, given that the *bif2* mutant phenotype could equally be interpreted as an absence of branch zone, the length of the branch zone may simply be a more sensitive metric of allelic differences at *bif2* than the number of tassel branches. More specifically, the range of natural allelic variation at *bif2* may not be sufficient to have a strong significant effect on tassel branch number, possibly because branch number is affected by so many other segregating mutations with much greater effects.

Epistatic interactions with *bif2* condition vegetative phenotypes

Linkage analysis in the IBM population reveals no main effect of *bif2* on plant height or node number, and the *bif2* mutant has no obvious vegetative phenotype. However, a genome scan for epistatic interactions with *bif2* reveals several epistatic QTL for node number (Table 3), in much the same way that combining the *bif2* mutation with mutations in other auxin-related loci, including *spi1* and *Bif1*, yields dramatic vegetative phenotypes. Neither of the genes previously identified as epistatic to *bif2* in mutant studies map to the epistatic QTL identified here: *spi1* maps to ctg146 on chromosome 3 (Gallavotti *et al.*, 2008b), and *Bif1* maps to bin 8.02 (Barazesh and McSteen, 2008). However, the epistatic QTL in bin 4.08 maps close to *ZmPIN1c* on ctg184 (http://www.maizesequence.org/), an obvious candidate for interaction with *bif2*, and the epistatic QTL in bin 5.04 maps to the same location as the uncloned mutant *Developmental disaster1* (*Dvd1*) which has short internodes and no tassel branches (P. McSteen, personal communication). It is important to recognize the difference between statistical epistasis, which is the identification of a significant interaction term in linkage, association, or other quantitative studies, and developmental epistasis, which is an interaction between biological components in a system (Brodie, 2000). Either kind of epistasis may exist without the other: two genes expressed in mutually exclusive tissues may still show evidence of statistical epistasis, and two subunits in a protein complex will not necessarily show statistical epistasis, most obviously if one of the subunits harbors no functional variation. However, knowledge of developmental epistasis can nevertheless inform the choice of candidate genes for epistatic QTL, and the presence of a *ZmPIN1c*-linked QTL epistatic with *bif2* for node number provides a compelling hypothesis for future investigation.

Association of the *bif2* locus with flowering time

Association mapping suggests an effect of *bif2* on flowering time that is corroborated by neither our linkage work nor previous mutagenesis studies. However, there is strong segregation distortion in favor of the B73 allele at the *bif2* locus in the IBM linkage population (Figure 4c). Preliminary analysis in the NAM linkage populations also suggests that *bif2* aligns with a QTL for the anthesis–silking interval (ASI; the delay between male and female reproductive maturity; data not shown). Since overlap between male and female reproductive timing is necessary for self-pollination and the maintenance of inbred lines, the inheritance bias against the Mo17 *bif2* allele may reflect a deleterious ASI effect. However, the fact that the Mo17 *bif2* allele is still found at a reasonably high frequency in both the IBM population and the association panel suggests that any deleterious effect may be mitigated by other genetic factors. For example, the mitigation of a deleterious ASI effect in early flowering genetic backgrounds would explain the association mapping result that implicates *bif2* in flowering time variation.

Possible mechanistic differences between *bif2* alleles

The B73 allele of *bif2* is associated with a longer tassel branch zone length and shows increased expression relative to the Mo17 allele in F_1 hybrid inflorescence meristem tissues, consistent with the fact that the *bif2* mutant (no expression) shows reductions in tassel branching (Figure 5). In the vegetative portion of the plant, the B73 allele of *bif2* is associated with increased height and node number below the primary ear, but additional genetic factors are required to generate the phenotype, and it is not known whether the B73 allele shows increased expression relative to the Mo17 allele in vegetative tissues. The molecular basis of the difference in *bif2* expression in the inflorescence could be transcriptional, reflecting *cis*-regulatory differences in the timing, amplitude, and/or spatial extent of *bif2* expression, or post-transcriptional, reflecting differences in transcript stability. *Cis*-regulatory differences could be caused by one of the sequence polymorphisms identified in the promoter region; for example, although the same TATA box appears

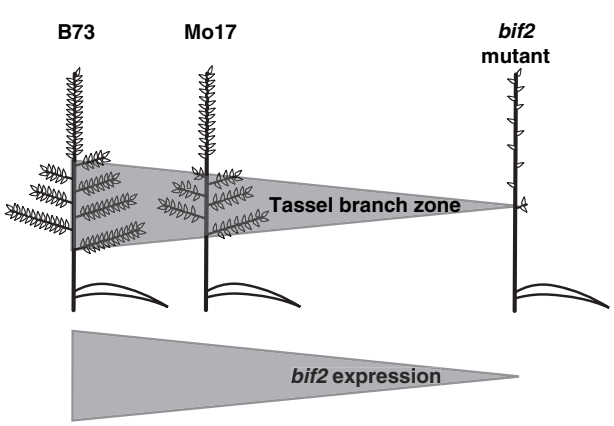

Figure 5. Tassel branch zone length is correlated with *bif2* expression.

to act as the promoter for both transcripts, B73 contains an extra copy of this motif (Figure 3). However, due to the low level of recombination observed across *bif2* we have little power to determine whether the causal polymorphism lies upstream, downstream, or within the coding region itself. For two previously cloned QTL in maize, *tb1* and *vgt1*, the causal polymorphisms were found to lie ~60 and ~70 kb upstream, respectively, of the genes whose expression they affect (Clark *et al.*, 2006; Salvi *et al.*, 2007). Similarly, the regulatory sequences responsible for paramutation at the maize B locus are ~100 kb upstream of the B gene (Stam *et al.*, 2002). Such difficulties have led some to question whether map-based cloning down to the causal quantitative trait nucleotide (QTN) is worthwhile, particularly when mutagenesis and association approaches have converged on a convincing candidate gene (Salvi and Tuberosa, 2005).

Combined mutant-quantitative analyses to identify polymorphisms underlying natural variation

The compilation of evidence from linkage, association, and mutagenesis approaches suggests that while knockdowns or knockouts of *bif2* function are either inflorescence-specific or have relatively mild vegetative phenotypes by themselves, *bif2* mutations in concert with other mutations that disrupt auxin homeostasis can generate effects on a range of vegetative and reproductive phenotypes, including traits of fundamental agronomic importance like plant height and flowering time. Mutagenesis and linkage mapping provide estimates of allelic effects within a narrow genetic background, and therefore detected *bif2* involvement in only a subset of the traits identified by association mapping. Association mapping provides a comprehensive overview of traits associated with allelic variation at a locus, but is of limited usefulness for understanding epistatic relationships with *bif2*, both because of multiple-testing constraints and because selection may have purged deleterious allelic combinations from the association panel, which is a collection of selected commercial inbreds. Together, these complementary approaches identified associations between the *bif2* locus and a broad range of traits in maize, suggesting that molecular variation in PIN/PID-based polar auxin transport may be widely responsible for architectural variation in maize and other species. Robertson's (1985) hypothesis states that the polymorphisms of small effect that underlie quantitative variation are not fundamentally different from the polymorphisms of large effect that underlie qualitative, or mutant, variation. This hypothesis is invoked every time mutant phenotypes are used to identify candidate genes for natural variation, yet it has been verified using only a few genes with large, qualitative allelic effects, including *tb1* in maize (Doebley *et al.*, 1995) and *CRY2* (El-Assal *et al.*, 2001) and *PHYA* (Maloof *et al.*, 2001) in Arabidopsis. The *bif2* alleles identified in this study have relatively minor effects, demonstrating that Robertson's hypothesis still holds for the small-effect alleles that represent the vast majority of functional polymorphisms in nature.

EXPERIMENTAL PROCEDURES

Sequencing of *bif2*

Two fragments representing 2.1 kb from the *bif2* locus were sequenced in a panel of 277 diverse maize lines. The first fragment represents a portion of the first exon and ~700 bp of upstream sequence. The second fragment represents a portion of the intron and the second exon. Sequence data were not obtained for a portion of the first exon and intron. The first fragment is 795 bp in B73 using primers (5′-TCCCCGACAAAGTTACCAGT-3′) and (5′-ACCTCGGTCACCGTCTTGTT-3′); the latter primer was used for the sequencing reaction. The second fragment was resequenced by Genaissance Pharmaceuticals (http://www.clda.com). The first fragment contains a miniature inverted repeat transposable element (MITE) insertion in some lines, including Mo17; this insertion was used to genotype the inter-mated B73 × Mo17 population at the *bif2* locus.

Phenotyping

The maize association panel was grown and evaluated in Raleigh, NC during the 2002 summer season; in Homestead, FL during the 2002–03 winter season; in Madison, WI, Columbia, MI and Raleigh, NC during the 2003 summer season; in Raleigh, NC (two complete reps), Columbia, MO, Aurora, NY, and Urbana, IL during the 2006 summer season and in Homestead, FL and Ponce, PR during the 2006–07 winter season. The IBM population was grown and evaluated in Raleigh, NC (two complete reps), Columbia, MO, Aurora, NY, and Urbana, IL during the 2006 summer season and in Homestead, FL and Ponce, PR during the 2006–07 winter season. Lines were evaluated for the 14 traits shown in Figure 1. Data used for analysis are the standardized averages.

Association mapping analysis

The mixed-model approach developed by Yu *et al.* (2006) was used to test for statistical association between phenotype and genotype in the association panel, using the same population structure (Q) and kinship (K) matrices derived by Yu *et al.* (2006). The test of SNP/QTN effect was carried out by *F* test, with denominator degrees of freedom per the Satterthwaite method, after the convergence of restricted maximum likelihood (REML) using a mixed model that accounted for both population structure and kinship (QK): $\boldsymbol{y} = \mathbf{X}\beta + \mathbf{S}\alpha + \mathbf{Q}\boldsymbol{v} + \mathbf{Z}\boldsymbol{u} + \boldsymbol{e}$. Here, $\boldsymbol{y}$ is a vector of phenotypic observation; α is a vector of allelic effects; $\boldsymbol{e}$ is a vector of residual effects; $\boldsymbol{v}$ is a vector of population effects; β is a vector of fixed effects other than allelic or population group effects; $\boldsymbol{u}$ is a vector of polygenic background effects; $\mathbf{Q}$ is the population membership assignment matrix (based on SSR genotypic data and calculated using *Structure*) relating $\boldsymbol{y}$ to $\boldsymbol{v}$; and $\mathbf{X}$, $\mathbf{S}$, and $\mathbf{Z}$ are incidence matrices of ones and zeros relating $\boldsymbol{y}$ to β, α, and $\boldsymbol{u}$, respectively. The variances of the random effects are expressed as $\mathrm{Var}(\boldsymbol{u}) = \mathbf{K}V_g$, and $\mathrm{Var}(\boldsymbol{e}) = \mathbf{R}V_R$, where $\mathbf{K}$ is the kinship matrix (based on SSR genotypic data and calculated using *SPAGeDi* 1.02; Hardy and Vekemans, 2002), $\mathbf{R}$ is a matrix with the off-diagonal elements being zero and the diagonal elements being the reciprocal of the number of observations for

which each phenotypic data point was obtained, V_g is the genetic variance, and V_R is the residual variance. Best linear unbiased estimates of β, α, and $\boldsymbol{v}$ (fixed effects), and best linear unbiased predictions of $\boldsymbol{u}$ (random effects) were obtained by solving the mixed-model equation.

QTL analysis

The GLMselect procedure in SAS 9.1 (SAS Institute, http://www.sas.com/) was used to identify QTL for the traits listed in Table 1 in the IBM population. Missing genotype data were set as intermediate (1.5) to the two parental alleles (1 and 2), and forward stepwise regression was performed with an entry/exit threshold of 0.0025. Those QTL unlinked to *bif2* were then set as cofactors for refinement of *bif2*-linked QTL positions (Figure 4a,b) and to conduct genome-wide scans for interaction with *bif2*. By testing only for interaction with *bif2*, the number of tests was limited to the number of markers.

Allele-specific expression assay

Measuring the relative allelic expression in heterozygotes provides a sensitive means of detecting within-sample regulatory differences while controlling for variation in developmental staging and the quality of cDNA between samples (Clark *et al.*, 2006). We exploited a 3-bp insertion–deletion (indel) polymorphism between B73 and Mo17 at the end of the second exon of *bif2* to examine the relative expression of *bif2* alleles in developing inflorescences (6–16 mm) of B73–Mo17 F_1 hybrids. Total RNA was extracted using TRIzol (Invitrogen, http://www.invitrogen.com/), treated overnight with DNase (Invitrogen), and DNase was removed with a phenol:chloroform extraction. The RNA samples were quantified using a ND-1000 (NanoDrop Technologies, http://www.nanodrop.com/), and 2 μg total RNA was used for first-strand cDNA synthesis using a poly-A primer, 200 U M-MLV reverse-transcriptase (Promega, http://www.promega.com/), and 40 U RNAsin (Promega). A FAM-labeled forward primer (5′-GGAGTACCTGCACATGATGGGCA-3′) and an unlabeled reverse primer (5′-GCTTCCCGGACCACCTGTTC-3′) were used to amplify 187-bp and 190-bp fragments from the B73 and Mo17 *bif2* transcripts, respectively. The PCR fragments were assayed on an ABI 3730 fragment analyzer, and peak areas were determined using GeneMapper 4.0. Four independent amplifications were performed on each biological sample. Two samples of B73–Mo17 F_1 genomic DNA were included in each technical replicate as controls, and the average 187/190 ratio of each sample was divided by the average 187/190 ratio of these controls. Confidence intervals (95%) for the expression ration were calculated as follows: $\mu \pm 1.96\sigma_\mu$ with $\sigma_\mu = \sigma/\sqrt{n}$ where μ is the mean of the B73/Mo17 expression ratios, σ_μ is the standard deviation of this mean, and σ is the standard deviation of the B73/Mo17 expression ratios and n the number of observations.

5′ and 3′ RACE

The GeneRacer kit (Invitrogen) was used to amplify 5′ and 3′ *bif2* cDNA ends using total RNA from ear meristems of B73–Mo17 F_1 plants. Reverse transcription was performed with SuperScript III (Invitrogen) and a poly-T oligo. Gene-specific primers used for cDNA amplification were (5′-GAACAGGTGGTCCGGGAAGC-3′) for 5′ RACE and (5′-GGAGTACCTGCACATGATGGGCA-3′) for 3′ RACE. Nested PCR was performed for 5′ RACE only using the (5′-CGACGGCGTCGACGTGCACTG-3′) primer reported by McSteen *et al.* (2007). The RACE products were transformed into the pCR4-TOPO vector (Invitrogen), cloned, and sequenced.

ACKNOWLEDGEMENTS

We would like to thank Paula McSteen for her thorough review of the initial manuscript and for providing the *bif2* sequence before it was made public. Research support was provided by NSF Plant Genome Grant DBI 0321467.

SUPPORTING INFORMATION

Additional Supporting Information may be found in the online version of this article:

Table S1. Genotype data and population structure assignments for the maize inbred lines used in this study.

Please note: Wiley-Blackwell are not responsible for the content or functionality of any supporting materials supplied by the authors. Any queries (other than missing material) should be directed to the corresponding author for the article.

REFERENCES

Barazesh, S. and McSteen, P. (2008) *Barren inflorescence1* functions in organogenesis during vegetative and inflorescence development in maize. *Genetics* **179**, 389–401.

Benjamins, R., Quint, A., Weijers, D., Hooykaas, P. and Offringa, R. (2001) The PINOID protein kinase regulates organ development in *Arabidopsis* by enhancing polar auxin transport. *Development*, **128**, 4057–4067.

Benkova, E., Michniewicz, M., Sauer, M., Teichmann, T., Seifertova, D., Jurgens, G. and Friml, J. (2003) Local, efflux-dependent auxin gradients as a common module for plant organ formation. *Cell*, **115**, 591–602.

Brodie, E.D. (2000) Why evolutionary genetics does not always add up. In *Epistasis and the Evolutionary Process* (Wolf, J.B., Brodie, E.D. and Wade, M.J., eds). Oxford: Oxford University Press, pp. 3–19.

Cheng, Y., Dai, X. and Zhao, Y. (2006) Auxin biosynthesis by the YUCCA flavin monooxygenases controls the formation of floral organs and vascular tissues in Arabidopsis. *Genes Dev.* **20**, 1790–1799.

Christensen, S.K., Dagenais, N., Chory, J. and Weigel, D. (2000) Regulation of auxin response by the protein kinase PINOID. *Cell*, **100**, 469–478.

Clark, R.M., Wagler, T.N., Quijada, P. and Doebley, J. (2006) A distant upstream enhancer at the maize domestication gene *tb1* has pleiotropic effects on plant and inflorescent architecture. *Nat. Genet.* **38**, 594–597.

Doebley, J., Stec, A. and Gustus, C. (1995) *teosinte branched1* and the origin of maize: evidence for epistasis and the evolution of dominance. *Genetics*, **141**, 333–346.

El-Assal, S.E.-D., Alonso-Blanco, C., Peeters, A.J., Raz, V. and Koornneef, M. (2001) A QTL for flowering time in Arabidopsis reveals a novel allele of CRY2. *Nat. Genet.* **29**, 435–440.

Flint-Garcia, S.A., Thornsberry, J.M. and Buckler, E.S. (2003) Structure of linkage disequilibrium in plants. *Annu. Rev. Plant Biol.* **54**, 357–374.

Flint-Garcia, S.A., Thuillet, A.C., Yu, J., Pressoir, G., Romero, S.M., Mitchell, S.E., Doebley, J., Kresovich, S., Goodman, M.M. and Buckler, E.S. (2005) Maize association population: a high-resolution platform for quantitative trait locus dissection. *Plant J.* **44**, 1054–1064.

Friml, J., Wisniewska, J., Benkova, E., Mendgen, K. and Palme, K. (2002) Lateral relocation of auxin influx regulator PIN3 mediates tropism in Arabidopsis. *Nature*, **415**, 806–909.

Friml, J., Vieten, A., Sauer, M., Weijers, D., Schwarz, H., Hamann, T., Offringa, R. and Jurgens, G. (2003) Efflux-dependent auxin gradients establish the apical-basal axis of Arabidopsis. *Nature*, **426**, 147–153.

Friml, J., Yang, X., Michniewicz, M. *et al.* (2004) A PINOID-dependent binary switch in apical-basal PIN polar targeting directs auxin efflux. *Science*, **306**, 862–865.

Fu, Y., Wen, T.-J., Ronin, Y.I. *et al.* (2006) Genetic dissection of intermated recombinant inbred lines using a new genetic map of maize. *Genetics*, **174**, 1671–1683.

Gallavotti, A., Zhao, Q., Kyozuka, J., Meeley, R.B., Ritter, M.K., Doebley, J.F., Pe, M.E. and Schmidt, R.J. (2004) The role of *barren stalk1* in the architecture of maize. *Nature*, **432**, 630–635.

Gallavotti, A., Yang, Y., Schmidt, R.J. and Jackson, D. (2008a) The relationship between auxin transport and maize branching. *Plant Physiol.* **147**, 1913–1923.

Gallavotti, A., Barazesh, S., Malcomber, S., Hall, D., Jackson, D., Schmidt, R.J. and McSteen, P. (2008b) *sparse inflorescence1* encodes a monocot-specific YUCCA-like gene required for vegetative and reproductive development in maize. *Proc. Natl Acad. Sci. USA*, **105**, 15190–15195.

Galweiler, L., Guan, C., Muller, A., Wisman, E., Mendgen, K., Yephremov, A. and Palme, K. (1998) Regulation of polar auxin transport by AtPIN1 in Arabidopsis vascular tissue. *Science*, **282**, 2226–2230.

Goldsmith, M.H.M. and Goldsmith, T.H. (1981) Quantitative predictions for the chemiosmotic uptake of auxin. *Planta*, **153**, 25–33.

Hardy, O.J. and Vekemans, X. (2002) SPAGeDi: a versatile compute program to analyze spatial genetic structure at the individual or population levels. *Mol. Ecol. Notes*, **2**, 618.

Heisler, M.G., Ohno, C., Das, P., Sieber, P., Reddy, G.V., Long, J.A. and Meyerowitz, E.M. (2005) Patterns of auxin transport and gene expression during primordium development revealed by live imaging of the Arabidopsis inflorescence meristem. *Curr. Biol.* **15**, 1899–1911.

Kempin, S.A., Savidge, B. and Yanofsky, M.F. (1995) Molecular basis of the cauliflower phenotype in Arabidopsis. *Science*, **267**, 522–525.

Kleine-Vehn, J., Dhonukshe, P., Sauer, M., Brewer, P.B., Wisniewska, J., Paciorek, T., Benkova, E. and Friml, J. (2008) ARF GEF-dependent transcytosis and polar delivery of PIN auxin carriers in *Arabidopsis*. *Curr. Biol.* **18**, 526–531.

Leyser, O. (2005) Auxin distribution and plant pattern formation: how many angels can dance on the point of PIN? *Cell*, **121**, 819–822.

Maloof, J.N., Borevitz, J.O., Dabi, T. *et al.* (2001) Natural variation in light sensitivity of Arabidopsis. *Nat. Genet.* **29**, 357–358.

McSteen, P. and Hake, S. (2001) *barren inflorescence2* regulates axillary meristem development in the maize inflorescence. *Development*, **128**, 2881–2891.

McSteen, P., Malcomber, S., Skirpan, A., Lunde, C., Wu, X., Kellogg, E. and Hake, S. (2007) *barren inflorescence2* encodes a co-ortholog of the PINOID serine/threonine kinase and is required for organogenesis during inflorescence and vegetative development in maize. *Plant Physiol.* **144**, 1000–1011.

Michniewicz, M., Zago, M.K., Abas, L. *et al.* (2007) Antagonistic regulation of PIN phosphorylation by PP2A and PINOID directs auxin flux. *Cell*, **130**, 1044–1056.

Orr, H.A. (1998) The population genetics of adaptation: the distribution of factors fixed during adaptive evolution. *Evolution*, **52**, 935–949.

Petrasek, J., Mravec, J., Bouchard, R. *et al.* (2006) PIN proteins perform a rate-limiting function in cellular auxin efflux. *Science*, **312**, 914–918.

Reinhardt, D., Pesce, E.-R., Stieger, P., Mandel, T., Baltensperger, K., Bennett, M., Traas, J., Friml, J. and Kuhlemeier, C. (2003) Regulation of phyllotaxis by polar auxin transport. *Nature*, **426**, 255–260.

Remington, D.L., Thornsberry, J.M., Matsuoka, Y., Wilson, L.M., Whitt, S.R., Doebley, J., Kresovich, S., Goodman, M.M. and Buckler, E.S. (2001) Structure of linkage disequilibrium and phenotypic association in the maize genome. *Proc. Natl Acad. Sci. USA*, **98**, 11479–11484.

Robertson, D.S. (1985) A possible technique for isolating genic DNA for quantitative traits in plants. *J. Theor. Biol.* **117**, 1–10.

Salvi, S. and Tuberosa, R. (2005) To clone or not to clone plant QTLs: present and future challenges. *Trends Plant Sci.* **10**, 297–304.

Salvi, S., Sponza, G., Morgante, M. *et al.* (2007) Conserved noncoding genomic sequences associated with a flowering-time quantitative trait locus in maize. *Proc. Natl Acad. Sci. USA*, **104**, 11376–11381.

Scarpella, E., Marcos, D., Friml, J. and Berleth, T. (2006) Control of leaf vascular patterning by polar auxin transport. *Genes Dev.* **20**, 1015–1027.

Skirpan, A., Wu, X. and McSteen, P. (2008) Genetic and physical interaction suggest that barren stalk1 is a target of barren inflorescence2 in maize inflorescence development. *Plant J.* **55**, 787–797.

Smith, R.S. (2008) The role of auxin transport in plant patterning mechanisms. *PLoS Biol.* **6**, e323.

Smith, R.S., Guyomarc'h, S., Mandel, T., Reinhardt, D., Kuhlemeier, C. and Prusinkiewicz, P. (2006) A plausible model of phyllotaxis. *Proc. Natl Acad. Sci. USA*, **103**, 1301–1306.

Stam, M., Belele, C., Dorweiler, J.E. and Chandler, V.L. (2002) Differential chromatin structure within a tandem array 100 kb upstream of the maize b1 locus is associated with paramutation. *Genes Dev.* **16**, 1906–1918.

Stern, D.L. (2000) Perspective: evolutionary developmental biology and the problem of variation. *Evolution*, **54**, 1079–1091.

Tanaka, H., Dhonukshe, P., Brewer, P.B. and Friml, J. (2006) Spatiotemporal asymmetric auxin distribution: a means to coordinate plant development. *Cell. Mol. Life Sci.* **63**, 2738–2754.

Thornsberry, J.M., Goodman, M.M., Doebley, J., Kresovich, S., Nielsen, D. and Buckler, E.S. (2001) Dwarf8 polymorphisms associate with variation in flowering time. *Nat. Genet.* **28**, 286–289.

Vieten, A., Vanneste, S., Wisniewska, J., Benkova, E., Benjamins, R., Beeckman, T., Luschnig, C. and Friml, J. (2005) Functional redundancy of PIN proteins is accompanied by auxin-dependent cross-regulation of PIN expression. *Development*, **132**, 4521–4531.

Wenzel, C.L., Schuetz, M., Yu, Q. and Mattsson, J. (2007) Dynamics of MONOPTEROS and PIN-FORMED1 expression during leaf vein pattern formation in *Arabidopsis thaliana*. *Plant J.* **49**, 387–398.

Wisniewska, J., Xu, J., Seifertova, D., Brewer, P.B., Ruzicka, K., Blilou, I., Rouquie, D., Benkova, E., Scheres, B. and Friml, J. (2006) Polar PIN localization directs auxin flow in plants. *Science*, **312**, 883.

Yu, J., Pressoir, G., Briggs, W.H. *et al.* (2006) A unified mixed-model method for association mapping accounting for multiple levels of relatedness. *Nat. Genet.* **38**, 203–208.

Yu, J., Holland, J.B., McMullen, M.D. and Buckler, E.S. (2008) Genetic design and statistical power of nested association mapping in maize. *Genetics*, **178**, 539–551.

